J|A|C|S COMMUNICATIONS

Published on Web 12/07/2009

Improved Injection in n-Type Organic Transistors with Conjugated Polyelectrolytes

Jung Hwa Seo,[†] Andrea Gutacker,[†,‡] Bright Walker,[†] Shinuk Cho,[†] Andres Garcia,[†] Renqiang Yang,[†] Thuc-Quyen Nguyen,[†] Alan J. Heeger,[†] and Guillermo C. Bazan*[,†]

Center for Polymers and Organic Solids, University of California, Santa Barbara, California 93106, and Bergische Universitaet Wuppertal, Makromolekulare Chemie, Wuppertal, Germany

Received October 4, 2009; E-mail: bazan@chem.ucsb.edu

Contact resistances at metal/semiconductor interfaces can limit the performance of organic thin-film transistors (OTFTs).[1] Optimal devices should display a linear dependence of the channel potential profile and negligible voltage drops at the electrodes. These conditions allow one to accurately determine charge carrier mobilities from device characteristics and lead to low turn-on threshold voltages. In the case of n-channel OTFTs, and in the absence of interfacial effects, the electron injection barrier (ϕ_e) can be estimated from the difference in the energies of the work function (WF) of the metal and the LUMO of the semiconductor.[2] High contact resistances are therefore obtained under these conditions when using stable high WF metals, such as Au.

Large ϕ_e values may be similarly encountered in polymer light emitting diodes (PLEDs),[3] and a variety of strategies have been implemented to lower the operating voltages. One approach incorporates a conjugated polyelectrolyte (CPE) electron transport/injection layer adjacent to the cathode.[4] Improved electron injection can result from (a) hole accumulation at an internal organic interface, (b) electric field screening due to ion migration, and (c) formation of a permanent dipole layer at the topmost organic surface. The relative participation of these effects depends on the device structure, i.e. the thicknesses of different layers, and the intrinsic energy levels of the material components.[5]

Here, we demonstrate that the insertion of CPEs beneath top-contact Au source/drain electrodes can be a very effective strategy for improving carrier injection in n-channel TFTs, provided that the thickness of the ion-containing layer is sufficiently thin to avoid complications associated with electric field redistribution. Scheme 1 shows the structures of the CPEs used in this study. They contain a poly[9,9-bis[6′-(*N*,*N*,*N*-trimethylammonium)hexyl]fluorene-*alt*-*co*-1,4-phenylene] backbone with fluoride (**PFN$^+$F$^-$**), bromide (**PFN$^+$Br$^-$**), or tetrakis(imidazoly)borate (**PFN$^+$BIm$_4^-$**) counterions. [6,6]-Phenyl-C_{61}-butyric acid methyl ester (**PCBM**) was chosen as the n-type semiconductor (Scheme 1b). As shown in Scheme 1c, the energy difference between the WF of Au and the LUMO of **PCBM** would lead to the absence of interfacial effects, i.e. surface dipoles,[7] to a ϕ_e of 0.7 eV. Using the same argument one can estimate that introducing a CPE layer would increase ϕ_e to 2.2 eV. We have used for these estimates a LUMO energy of −4.2 eV, which is on the high end of the values provided in the literature (−3.7 to −4.3 eV) and anticipated to yield a *smaller* ϕ_e.[8]

CPE function was tested using the OTFT structure shown in Figure 1a. **PCBM** films of 35 nm thickness were deposited by spin-casting from a 1% (w/v) chloroform solution onto a SiO_2 gate insulator. The CPE layer was subsequently spin-cast from either 0.02% or 0.5% (w/v) methanol solutions. Profilometry showed that the 0.5% solutions provided CPE layers on the order of ∼15−20 nm thickness, which were smooth, as determined by atomic force microscopy (AFM, see Supporting Information (SI)). No significant increase in the total thickness of the organic layer was observed when the more dilute solution was used. However, X-ray photoelectron spectroscopy (XPS) analysis of these surfaces shows N 1s features at ∼403 eV due to quaternized *N*-C functionalities.[5b] Water contact angle measurements are also consistent with a more hydrophilic surface (SI). Therefore, dilute solutions do not yield well-defined layers, but one can nonetheless deposit CPE on top of **PCBM**. The final step in device construction involves thermal evaporation of 50 nm thick Au electrodes.

Scheme 1. Structures of (a) CPEs and (b) **PCBM**, and (c) Energy Level Diagram of **PCBM**, CPE, and Au As Obtained by UPS[5b,6]

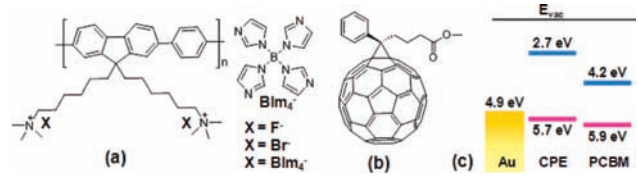

Figure 1b displays the transfer characteristics with a positive gate bias, which leads to an n-type device. Despite the nearly absent change in total film thickness, CPE deposition from dilute solution leads to OTFTs with higher drain currents (I_{DS}), relative to untreated **PCBM**. Table 1 provides a summary of relevant device characteristics, including field-effect mobilities (μ), current on−off ratios (I_{on}/I_{off}), and threshold voltages (V_{th}).

The data in Table 1 demonstrate that devices treated with dilute CPE solutions exhibit average values of $\mu \approx 10^{-2}$ cm^2/V·s, $I_{on}/I_{off} \approx 10^5$, and $V_{th} \approx 1$ V and that the nature of the counteranions bears

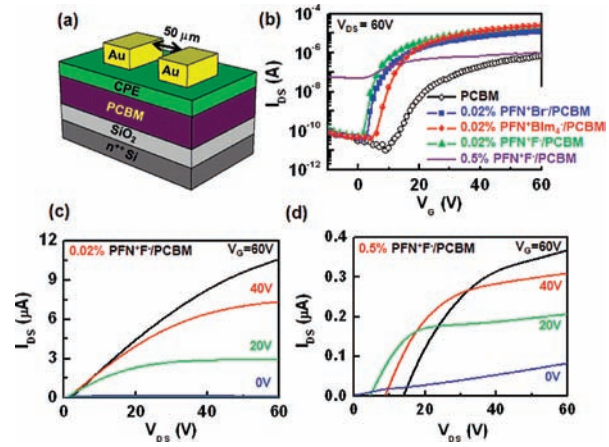

Figure 1. (a) OTFT test device. (b) Transfer characteristics at $V_{DS} = 60$ V as a function of counterion and concentration (for only **PFN$^+$F$^-$**). (c, d) Output characteristics with **PFN$^+$F$^-$** layers deposited from 0.02% and 0.5% methanol solutions, respectively.

[†] University of California.
[‡] Bergische Universitaet Wuppertal.

10.1021/ja908441c © 2009 American Chemical Society

Table 1. Typical Device Characteristics

	PCBM	0.02% PFN^+Br^-/ PCBM	0.02% $PFN^+Blm_4^-$/ PCBM	0.02% PFN^+F^-/ PCBM	0.5% PFN^+F^-/ PCBM
μ ($cm^2/V\cdot s$)	2.99×10^{-3}	1.00×10^{-2}	1.28×10^{-2}	1.24×10^{-2}	2.33×10^{-3}
I_{on}/I_{off}	3.16×10^4	4.42×10^5	5.41×10^5	3.48×10^5	1.41×10^1
V_{th} (V)	17.6 ± 3	1.82 ± 1	0.89 ± 1	1.07 ± 1	–

only a small influence on the device performance. The mobilities are comparable to those of **PCBM** OTFTs on bare SiO_2 with low WF electrodes (Al and Ca).[1d,9] Improved injection of electrons across the metal/organic interface when the CPE is deposited in small quantities is therefore demonstrated.

From Figure 1c, the output characteristics of thin **PFN^+F^-/PCBM** devices show clear saturation of I_{DS} at the region of larger V_{DS}. Examination of the transfer (Figure 1b) and output (Figure 1d) characteristics of OTFTs with the thicker 20 nm CPE layer reveals higher off currents and lower I_{on}/I_{off} ratios. Close examination of Figure 1d reveals (a) negative currents (*i.e.* $I_{DS} \neq 0$ when $V_{DS} = 0$), which suggest leakage through the gate dielectric and thus affect parameter extraction (Table 1), and (b) an increase of I_{DS} with V_{DS}, when $V_G = 0$ V (blue trace), indicating additional bulk current in the ~20 nm CPE layer. The unsaturated current at $V_G = 0$ V and shifting of the $I-V$ characteristics suggest ion motion within the CPE layer.[10] These conditions may lead to modifications of the electric fields away from the most desirable conditions and a corresponding loss of device performance.

Now we consider only devices fabricated by using dilute CPE solutions. Measurements of the total resistance (R_{total}) between the source and drain electrodes were performed for a series of different channel lengths (L). The R_{total} values were obtained from the linear portion of the output characteristics with $V_G = 60$ V. Taking into account that the channel resistance scales with L, one can estimate the contact resistance (R_c) from the extrapolation of R_{total} *vs* L to zero channel length (see Figure 2a). From these plots one finds a substantial decrease of R_c, from 13.5 MΩ for **PCBM** to 0.42 MΩ for **PFN^+F^-/PCBM**.

Ultraviolet photoelectron spectroscopy (UPS) was used to probe the energy levels of **PCBM** and the CPE. The anticipated ϕ_e was then estimated by the difference between the Fermi level (E_F) of Au and the LUMO of the organic semiconducting surface, as obtained by considering the UPS-determined HOMO (the highest occupied molecular orbital) energy level and the optical gap (E_g).[11] The results show that ϕ_e decreases after inserting the CPE injection layers (from 0.38 eV for **PCBM**/Au) to 0.03 eV for **PFN^+F^-/PCBM**, 0.04 eV for **PFN^+Br^-/PCBM**, and 0.01 eV for **$PFN^+BIm_4^-$/PCBM**, respectively. This smaller ϕ_e is suggested to account for the decrease in R_c.

From the UPS results, the thin CPE layer causes a downward shift of the vacuum level and, thereby, a lowering of the LUMO energy and the reduction in ϕ_e; see Figure 2b. Such an effect can be expected for an aligned interfacial dipole layer directed from the metal to the organic semiconductor. This geometry can be achieved with the hydrophobic CPE backbone preferentially interacting with the underlying **PCBM** and the concomitant positioning of the ionic component, such that the anions are accumulated at the topmost organic surface.[12]

In conclusion, a thin CPE layer can be used to lower the contact resistance in OTFTs. It is possible therefore to use high WF metals as electrodes in n-type devices. Our current thinking is that the CPE introduces interfacial dipoles at metal/organic semiconductor interfaces that modify the energy level alignment and improve

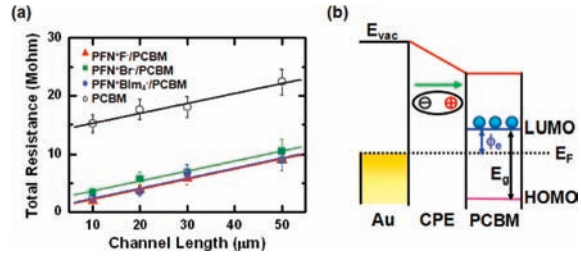

Figure 2. (a) Device resistance (R) from $I_{DS}-V_{DS}$ curves ($0 < V_{DS} < 10$ V, $V_G = 60$ V) with **PCBM** and 0.02% **CPE/PCBM** and different channel lengths. (b) Schematic energy levels in the presence of an interfacial dipole.

charge injection. Devices with smaller contact resistances and V_{th} values are therefore obtained. Care needs to be taken so that a CPE film does not interfere with the desired transistor gating behavior. This situation is observed with thicker films, where ion motion can redistribute electric fields and in which charge carrier transport along the CPE is a possibility.

Acknowledgment. The authors thank the NSF (DMR 0547639, 0606414, and 0602280) for financial support. We are grateful to Sarah R. Cowan and Dr. Jacek Brzezinski for assistance.

Supporting Information Available: Device fabrication details and characterization data. This material is available free of charge via the Internet at http://pubs.acs.org.

References

(1) (a) Natali, D.; Fumagalli, L.; Sampietro, M. *J. Appl. Phys.* **2007**, *101*, 014501. (b) Scheinert, S.; Paasch, G. *J. Appl. Phys.* **2009**, *105*, 014509. (c) Boudinet, D.; Blevennec, G. L.; Serbutoviez, C.; Verilhac, J.-M.; Yan, H.; Horowitz, G. *J. Appl. Phys.* **2009**, *105*, 084501. (d) Cho, S.; Seo, J. H.; Lee, K.; Heeger, A. J. *Adv. Funct. Mater.* **2009**, *19*, 1459.
(2) (a) Yan, H.; Chen, Z.; Zheng, Y.; Newman, C.; Quinn, J. R.; Dötz, F.; Kastler, M.; Facchetti, A. *Nature* **2009**, *457*, 679. (b) Chua, L.-L.; Zaumseil, J.; Chang, J.-F.; Ou, E. C.-W.; Ho, P. K.-H.; Sirringhaus, H.; Friend, R. H. *Nature* **2005**, *434*, 194. (c) Newman, C. R.; Frisbie, C. D.; da Silva Filho, D. A.; Brédas, J.-L.; Eqbank, P. C.; Mann, K. R. *Chem. Mater.* **2004**, *16*, 4436.
(3) (a) Brewer, P. J.; Lane, P. A.; deMello, A. J.; Bradley, D. D. C.; deMello, J. C. *Adv. Funct. Mater.* **2004**, *14*, 562. (b) Niu, X.; Qin, C.; Zhang, B.; Yang, J.; Xie, Z.; Cheng, Y.; Wang, L. *Appl. Phys. Lett.* **2007**, *90*, 203513. (c) Huang, Q.; Evmenenko, G. A.; Dutta, P.; Lee, P.; Armstrong, N. R.; Marks, T. J. *J. Am. Chem. Soc.* **2005**, *127*, 10227.
(4) (a) Huang, F.; Wu, H.; Wang, D.; Yang, W.; Cao, Y. *Chem. Mater.* **2004**, *16*, 708. (b) Gong, X.; Wang, S.; Moses, D.; Bazan, G. C.; Heeger, A. J. *Adv. Mater.* **2005**, *17*, 2053.
(5) (a) Hoven, C. V.; Yang, R.; Garcia, A.; Crockett, V.; Heeger, A. J.; Bazan, G. C.; Nguyen, T. -Q. *Proc. Nat. Acad. Sci. U.S.A.* **2008**, *105*, 12730. (b) Seo, J. H.; Yang, R.; Brzezinski, J. Z.; Walker, B.; Bazan, G. C.; Nguyen, T.-Q. *Adv. Mater.* **2009**, *21*, 1006.
(6) Akaike, K.; Kanai, K.; Yoshida, H.; Tsutsumi, J.; Nishi, T.; Sato, N.; Ouchi, Y.; Seki, K. *Appl. Phys. Lett.* **2008**, *104*, 023710.
(7) Mihailetchi, V. D.; Blom, P. W. M.; Hummelen, J. C.; Rispens, M. T. *J. Appl. Phys.* **2003**, *94*, 6849.
(8) Reese, M. O.; White, M. S.; Rumbles, G.; Ginley, D. S.; Shaheen, S. E. *Appl. Phys. Lett.* **2008**, *92*, 053307.
(9) (a) Lee, T.-W.; Byun, Y.; Koo, B.-W.; Kang, I.-N.; Lyu, Y.-Y.; Lee. C, H.; Pu, L.; Lee, S. Y. *Adv. Mater.* **2005**, *17*, 2180. (b) Tiwari, S. P.; Namdas, E. B.; Rao, V. R.; Fichou, D.; Mhaisalkar, S. G. *IEEE Electron Device Lett.* **2007**, *28*, 880. (c) Waldauf, C.; Schilinsky, P.; Perisutti, M.; Hauch, J.; Brabec, C. J. *Adv. Mater.* **2003**, *15*, 2084.
(10) (a) Edman, L.; Pauchard, M.; Liu, B.; Moses, D.; Heeger, A. J. *Appl. Phys. Lett.* **2003**, *82*, 3961. (b) Hepp, A.; Heil, H.; Schmechel, R.; Seggern, H. V. *Adv. Eng. Mater.* **2005**, *7*, 957.
(11) (a) Ishii, H.; Sugiyama, K.; Ito, E.; Seki, K. *Adv. Mater.* **1999**, *11*, 605. (b) Marmont, P.; Battaglini, N.; Lang, P.; Horowitz, G.; Hwang, J.; Kahn, A.; Amato, C.; Calas, P. *Org. Electron.* **2008**, *9*, 419. (c) Salaneck, W. R.; Lögdlund, M.; Fahlman, M.; Greczynski, G.; Kugler, Th. *Mater. Sci. Eng. R* **2001**, *34*, 121.
(12) (a) Li, H.; Xu, Y.; Hoven, C. V.; Li, C.; Seo, J. H.; Bazan, G. C. *J. Am. Chem. Soc.* **2009**, *131*, 8903. (b) Park, J.; Yang, R.; Hoven, C. V.; Garcia, A.; Fischer, D. A.; Nguyen, T.-Q.; Bazan, G. C.; DeLongchamp, D. M. *Adv. Mater.* **2008**, *20*, 2491.

JA908441C